

## **4. SHAFT SENSORLESS FORCED DYNAMICS CONTROL OF RELUCTANCE SYNCHRONOUS MOTOR DRIVES**

### **4.1. VECTOR CONTROLLED RELUCTANCE SYNCHRONOUS MOTOR DRIVES WITH PRESCRIBED CLOSED-LOOP SPEED DYNAMICS**

**Abstract:** A new speed control system for electric drives employing reluctance synchronous motors (RSM) is presented. The basic control system is similar to that presented in section 3 for PMSM, but for completeness of the presentation, some repetition is entailed. The usual vector control method is complemented with forced dynamic control instead of the PI control found in conventional drives. This initial study is restricted to speed control with the linear first order dynamic mode in which the closed-loop system response is first order with a pole location chosen by the user. To improve robustness of the closed-loop performance, an outer control loop based on model reference adaptive control (MRAC) is added. Simulation results presented show good correspondence with the theory and predict substantial robustness improvements with the aid of MRAC.

#### **4.1.1 Introduction**

In contrast to conventional approaches to electric drive control, a new control strategy for reluctance synchronous motors (RSM) is presented based on forced dynamic control (FDC). The combined RSM and load are viewed as a multivariable plant, the *control*, *measurement* and *controlled* variables being, respectively, the *stator voltages*, the *stator currents*, and the *rotor speed*. Like the systems described in previous chapters, a current control loop is closed via the power electronic switches so that the stator current demands become the control variables for the FDC based speed control loop. *This embodies RSM vector control [1] and generates automatically* stator current demands such that the rotor speed responds to the speed demand with the prescribed dynamics of the selected dynamic mode (ref., Chapter 1) which, in this case is the linear first order mode.

The new RSM drive control system embodies the block control principle [2], the motion separation principle [3] and sliding mode control [4].

The new RSM control system comprises two parts: a) the control law comprising *master* and *slave* control laws arranged in a hierarchical structure [2] and b) the state estimation and filtering system, comprising a complementary set of two observers, one used for reconstruction of the rotor speed, and the other for external load torque estimation [5]. Fig.4.1.1 shows the control system structure and its operation, the individual blocks being fully explained in the following sections. As in the previously described IM and PMSM drives, this drive may be included as an actuator in a larger scale control scheme to which linear control system design methods can be applied.

The same approach has also been investigated for permanent magnet synchronous motor drives [5], [6] and preliminary experimental results were presented in [7]. The master control law is operated in the *linear first order dynamic mode* in which *the rotor speed is controlled with linear, first order closed-loop dynamics, the closed-loop time constant being chosen by the control system designer*. In this initial investigation, the motor is assumed to drive a rigid body inertial load with moment of inertia,  $J$ , zero friction and subject to a constant external load torque,  $\Gamma_{Le}$ .

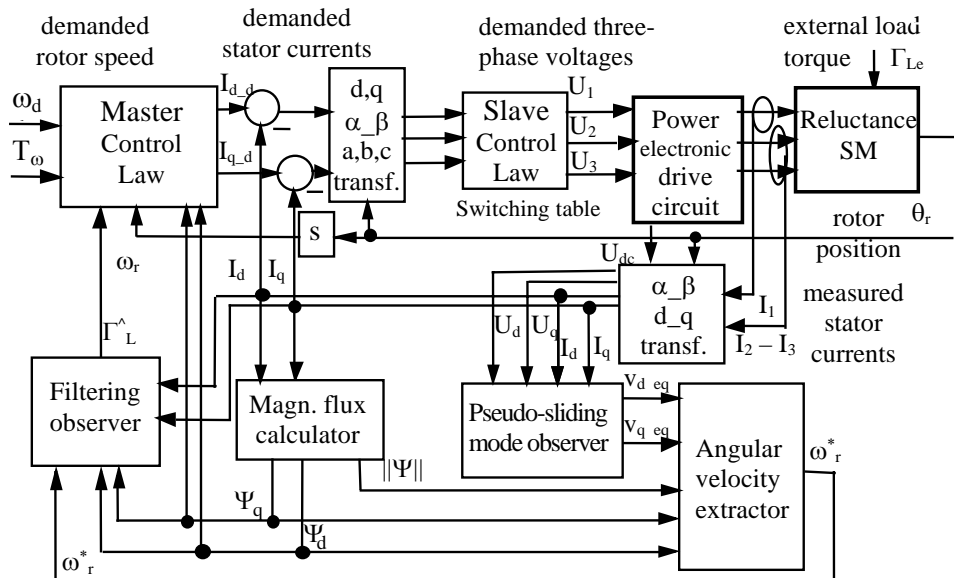


Fig. 4.1.1 Overall control system block diagram

## 4.1.2 Control System Development

### 2a) Model of Motor and Load

The following set of non-linear differential equations formulated in the rotating  $d, q$  co-ordinate system, coupled to the rotor, describe the RSM and form the basis of the control system development:

$$\mathbf{u}_s = R_s \mathbf{i}_s + \frac{d}{dt} \Psi_s + j\omega_r \Psi_s \quad (4.1.1)$$

$$J \frac{d\omega_r}{dt} = \frac{3p}{2} (\Psi_d i_q - \Psi_q i_d) - \Gamma_L = c_5 (L_d - L_q) i_d i_q - \Gamma_L, \quad (4.1.2)$$

where,  $\mathbf{i}_s = i_d + j i_q$ ,  $\mathbf{u}_s = u_d + j u_q$  and  $\Psi_s = \Psi_d + j \Psi_q$  are, respectively, the stator current, stator voltage and magnetic flux,  $\omega_r$  is the rotor velocity,  $p$  is the number of stator winding pole pairs,  $\Gamma_L$  is the external load torque,  $R_s$  is the phase resistance,  $L_d$  and  $L_q$  are the direct and quadrature phase inductances and  $c_5 = 3p/2$ . The ALA (*axially laminated anisotropic material*) RSM parameters assumed in this study are listed in the Appendix. The last term in (4.1.2) is obtained by noting that the magnetic flux components are given by  $\Psi_d = L_d(i_d)$  and  $\Psi_q = L_q(i_q)$ .

### 2b) Master control law

The basic philosophy of the forced dynamic control law development is the formulation of *linearising functions*, in this case embodying vector control, which *force* the nonlinear plant (i.e., the RSM and its load) to obey specified linear closed-loop differential equations, which in this case is a first order equation for the rotor speed yielding a dynamic response to a demanded speed,  $\omega_d(t)$ , with a prescribed time constant,  $T_\omega$ . The rotor speed therefore is made to satisfy:

$$\frac{d\omega_r}{dt} = \frac{1}{T_\omega} (\omega_d - \omega_r). \quad (4.1.3)$$

The rotor speed linearising function is chosen to force the non-linear differential equation (4.1.2) to have the same response as the linear equation (4.1.3). The linearising function is obtained simply by equating the right hand sides of (4.1.2) and (4.1.3), as follows:

$$\frac{1}{J} \left[ c_5 (\Psi_d i_q - \Psi_q i_d) - \Gamma_L \right] = \frac{1}{T_\omega} (\omega_d - \omega_r). \quad (4.1.4)$$

In the control law to be derived, estimates of the magnetic flux components,  $\Psi_d$  and the  $\Psi_q$  are evaluated from the known stator currents,  $i_d$  and  $i_q$ , by the magnetic flux calculator which takes into account the variations of the direct inductance,  $L_d$  as a function of the current,  $i_d$ , in the direct axis (*see Appendix*) while the quadrature inductance,  $L_q$ , is taken as a constant:

$$\Psi_d = L_d(i_d) \cdot i_d \quad \text{and} \quad \Psi_q = L_q i_q. \quad (4.1.5)$$

Mathematically, there are infinitely many combinations of  $i_d$  and  $i_q$  that may be chosen to satisfy (4.1.4). This enables the first part of the control law to be formulated on the basis of vector control [1]. Two vector control options will be presented. The first ensures that the maximum torque per unit of stator current is obtained. This requires the maximum practicable constant value,  $i_{dK}$ , of the stator current component,  $i_d$ , up to the base speed and not to allow its reduction under the prescribed value when the RSM is idle running. Above the base speed,  $i_d$  is reduced to ensure correct operation of the control system is maintained by keeping the magnitude of the back e.m.f. below the d.c. link voltage. Thus:

$$i_d = i_{dK}^* = \begin{cases} i_{dK} & \text{for } \omega_r < \omega_{\text{base}} \\ i_{dK} \frac{\omega_{\text{base}}}{|\omega_r|} & \text{for } \omega_r \geq \omega_{\text{base}} \end{cases} \quad (4.1.6a)$$

Alternatively, for maximum power factor the current,  $i_d$  can be determined from (4.1.6b) as:

$$i_d = \sqrt{\frac{\frac{J}{T_\omega} (\omega_d - \omega_r) + \Gamma_L}{c_5 (L_d - L_q) \tan \delta}}, \quad (4.1.6b)$$

where  $\delta$  is the angle of current vector in d, q system. Equation (4.1.6b) is based on a standard condition for maximum power factor for RSM [1] in which the motor is assumed to rotate at constant speed in one direction, and so the term,  $\frac{J}{T_\omega}(\omega_d - \omega_r) + \hat{\Gamma}_L$ , would not go negative. The fact that it can do so in the drive control system presented is taken into account in the formulation of the master control law below.

The master control law generates the *demanded* values of  $i_d$  and  $i_q$ , which will be denoted respectively by  $i_{d\_d}$  and  $i_{q\_d}$ , on the assumption that the inner current control loop (slave control law) ensures that  $i_d \cong i_{d\_d}$  and  $i_q \cong i_{q\_d}$ . Equation (4.1.6a) or equation (4.1.6b) are then used to evaluate  $i_{d\_d}$  and then equation (4.1.4) is solved for  $i_{q\_d}$ , yielding the second part of the master control law. Thus, using the flux estimates from equation (4.1.5), and the load torque estimate,  $\hat{\Gamma}_L$ , from the observer of section 3.2, the following master control laws are derived, one for each of the two vector control options:

a) for maximum torque per unit of stator current:

$$\begin{aligned} i_{d\_d} &= i_{dK}^* \\ i_{q\_d} &= \frac{\frac{\tilde{J}}{T_\omega}(\omega_d - \hat{\omega}_r) + \hat{\Gamma}_L}{c_5(\tilde{L}_d - \tilde{L}_q)} i_{dK}^* \end{aligned} \quad (4.1.7a)$$

b) for maximum power factor:

$$\begin{aligned} i_{d\_d} &= \sqrt{\left| \frac{\frac{\tilde{J}}{T_\omega}(\omega_d - \hat{\omega}_r) + \hat{\Gamma}_L}{c_5(\tilde{L}_d - \tilde{L}_q) \tan(\delta)} \right|} \\ i_{q\_d} &= i_{d\_d} \tan(\delta) \end{aligned} \quad (4.1.7b)$$

The estimates of all constant parameters,  $p$ , used in any model-based control law cannot be known with infinite precision, and are therefore denoted by  $\tilde{p}$  as for the control laws derived in the previous chapters.

## 2c) The slave control law

The slave control law closes the stator current control loop and is the same as in all the drive control systems presented in the previous chapters. The sub-plant to be controlled here is defined by equation (4.1.1), the control variables now being  $u_d$  and  $u_q$  and the output variables  $i_d$  and  $i_q$  to respond to the demanded currents  $i_{d,d}$  and  $i_{q,d}$ . The slave control law is the following *bang-bang control law*:

$$u_j = U_s \operatorname{sgn}(i_{j,d} - i_j), j = a, b, c, \quad (4.1.8)$$

where generally the transformations between the d, q components of the stator currents and voltages and the corresponding three-phase stator voltages and currents are given by:

$$\begin{bmatrix} z_d \\ z_q \end{bmatrix} = \begin{bmatrix} C & S \\ -S & C \end{bmatrix} \cdot \begin{bmatrix} 2/3 & -1/3 & -1/3 \\ 0 & 1/\sqrt{3} & -1/\sqrt{3} \end{bmatrix} \cdot \begin{bmatrix} z_1 \\ z_2 \\ z_3 \end{bmatrix}. \quad (4.1.9)$$

A special starting algorithm with constant current  $i_d$  and  $i_q$  demands comes into play while the magnetic flux norm,  $\|\Psi\|$ , builds up and control is handed over to the master control law of the previous section only once  $\|\Psi\|$  has risen above a pre-set minimum threshold. As in the previous drive control systems presented, the magnetic flux norm is defined as:

$$\|\Psi\| = \Psi_d^2 + \Psi_q^2. \quad (4.1.10)$$

### 4.1.3 State Estimation and Filtering

The load torque estimate, which is necessary for the master control algorithm is gained in a similar way to that of [5] and [6] for synchronous motor drives. First, a stator current vector *pseudo sliding-mode* observer is formulated for generation of an unfiltered estimate of the rotor speed. Second, the load torque estimate required by the master control law is provided by a standard observer having a similar structure to a Kalman filter, a direct measurement of load torque being assumed to be unavailable. It should be noted here that this load torque and filtered speed observer is identical in form for all the drive control systems, but the electrical torque input to the real time model is calculated using a different equation for each type of motor.

### 3a) The pseudo sliding mode observer and angular velocity extractor

The real time model of the system is based on the stator current equation (4.1.1) fed by the measured stator voltages and stator currents, but *purposely using only the terms without the rotor speed*,  $\omega_r$ . Thus:

$$\frac{d}{dt} \begin{bmatrix} i_d^* \\ i_q^* \end{bmatrix} = \begin{bmatrix} \frac{1}{\tilde{L}_d} & 0 \\ 0 & \frac{1}{\tilde{L}_q} \end{bmatrix} \cdot \begin{bmatrix} u_d \\ u_q \end{bmatrix} - \begin{bmatrix} \frac{R_s}{L_d} & 0 \\ 0 & \frac{R_s}{L_q} \end{bmatrix} \cdot \begin{bmatrix} i_d^* \\ i_q^* \end{bmatrix} + \begin{bmatrix} v_{eqd} \\ v_{eqq} \end{bmatrix} \quad (4.1.11)$$

where  $v_{eqd}$  and  $v_{eqq}$  are the model corrections and  $i_d^*$  and  $i_q^*$  are estimates of  $i_d$  and  $i_q$  as in a conventional observer. The useful observer outputs of the classical sliding mode observer would be the continuous *equivalent values* of the rapidly switching variables:

$$\begin{bmatrix} v_{eqd} \\ v_{eqq} \end{bmatrix} = V_{\max} \operatorname{sgn} \begin{bmatrix} i_d - i_d^* \\ i_q - i_q^* \end{bmatrix}. \quad (4.1.12)$$

Rather than compute this using a low pass filter, a *pseudo-sliding-mode* observer may be formed to obtain close approximations to  $v_{eqd}$  and  $v_{eqq}$  by replacing equation (4.1.12) with (4.1.13):

$$\begin{bmatrix} v_{eqd} \\ v_{eqq} \end{bmatrix} = K_{sm} \begin{bmatrix} i_d - i_d^* \\ i_q - i_q^* \end{bmatrix}, \quad (4.1.13)$$

where the gain,  $K_{sm}$ , is made as high as possible within the stability limit set by the sampling time of the digital processor. For large  $K_{sm}$ , the errors between real motor currents and fictitious observer currents are driven almost to zero, resulting in (4.1.14):

$$\begin{bmatrix} v_{eqd} \\ v_{eqq} \end{bmatrix} = \begin{bmatrix} 0 & p\omega_r^* \frac{\tilde{L}_q}{\tilde{L}_d} \\ -p\omega_r^* \frac{\tilde{L}_d}{\tilde{L}_q} & 0 \end{bmatrix} \cdot \begin{bmatrix} i_d \\ i_q \end{bmatrix}. \quad (4.1.14)$$

The right hand side contains the terms involving  $\omega_r$  that were omitted from the real-time model. An unfiltered rotor speed estimate,  $\omega_r^*$ , can then be ‘extracted’ from

equation (4.1.14). The component,  $v_{eq\ q}$  of (4.1.14), has been found to have lower noise levels than  $v_{eq\ d}$  and is therefore used alone to generate  $\omega_r^*$  :

$$\omega_r^* = \frac{-\tilde{L}_q v_{eq\ q}}{p\tilde{L}_d i_d} . \quad (4.1.15)$$

### 3b) The Load Torque Observer

Simple direct means of measuring the external load torque,  $\Gamma_L$  are not available. This is estimated by an observer that is identical in basic form to those of the drive control systems presented in the previous chapters. The details are given again in the interests of self-containment of this chapter and the fact that the electrical torque equation differs from one motor type to the next.

The problem of load torque estimation is easily solved by treating  $\Gamma_L$  as a state variable and including its estimate in the real time model of an observer. If the stator current measurement noise is significant, then the system performance will be improved by using the angular velocity estimate,  $\hat{\omega}_r$ , from the observer, which is a *filtered* version of  $\omega_r^*$ . The observer presented produces this filtered angular velocity estimate, without introducing a dynamic lag, which would impair the control system performance, in a similar fashion to a Kalman filter. The observer produces also a filtered rotor speed estimate and this is used in the control algorithm as well as the load torque estimate.

The real time model of the observer is based on torque equation (4.1.2). The observer correction loop is actuated by the error between the rotor speed estimate,  $\hat{\omega}_r$ , from the angular velocity extractor of the previous section and the estimate,  $\hat{\omega}_r$ , from the real time model:

$$\begin{aligned} e_\omega &= \omega_r^* - \hat{\omega}_r \\ \dot{\hat{\omega}}_r &= \frac{1}{T} \left[ c_5 (\Psi_d i_q - \Psi_q i_d) - \hat{\Gamma}_L \right] + k_\omega e_\omega \\ \dot{\hat{\Gamma}}_L &= k_\Gamma e_\omega \end{aligned} \quad (4.1.16)$$



Since  $\hat{\omega}_r$  is a filtered version of  $\omega_r^*$  it is used directly in the master control law. This is a conventional second order linear observer with a correction loop characteristic polynomial, which may be chosen via the gains,  $k_\omega$  and  $k_r$ , to yield the desired balance of filtering between the noise from the measurements of the currents  $i_d$  and  $i_q$  and the noise from the velocity measurement,  $\omega_r^*$ .

#### 4.1.4 Model Reference Control Based Outer Loop

To improve the robustness of the drive control system described in the previous sections an outer control loop based on model reference adaptive control (MRAC) may be formed. This is identical to that presented for the PMSM drive and so the reader is referred to section 3.2.3 for this.

#### 4.1.5 Simulation Results

All the simulation results are presented in Fig. 4.1.2, Fig. 4.1.3, Fig.4.1.4 and Fig. 4.1.5. They were carried out with a computational step of  $\Delta t=5e-5$  s, which corresponds to a sampling frequency of 20 kHz for digital implementation.

All the simulations are carried out with zero initial state variables and a step rotor speed demand of  $\omega_d = 100$  rad/s. A step external load torque of  $\Gamma_L=2,5$  Nm equal to the nominal motor torque is applied at  $t = 0,2$  [s], being zero for time interval  $0 \leq t < 0,2$  s. The response of the new basic forced dynamic control system operating in the linear first order dynamic mode is simulated first to illustrate the operation with the two alternative vector control options of the master control law defined by equations (4.1.7a) and (4.1.7b). The results are shown in Fig. 4.1.2 for maximum torque per unit stator current ( $i_d = \text{const}$ ) and in Fig. 4.1.4 for  $i_d$  controlled to yield the maximum power factor. These are then compared with the corresponding responses of the same control system augmented by a MRAC based outer loop and the simulation are shown in Fig. 4.1.3 and Fig. 4.1.5.

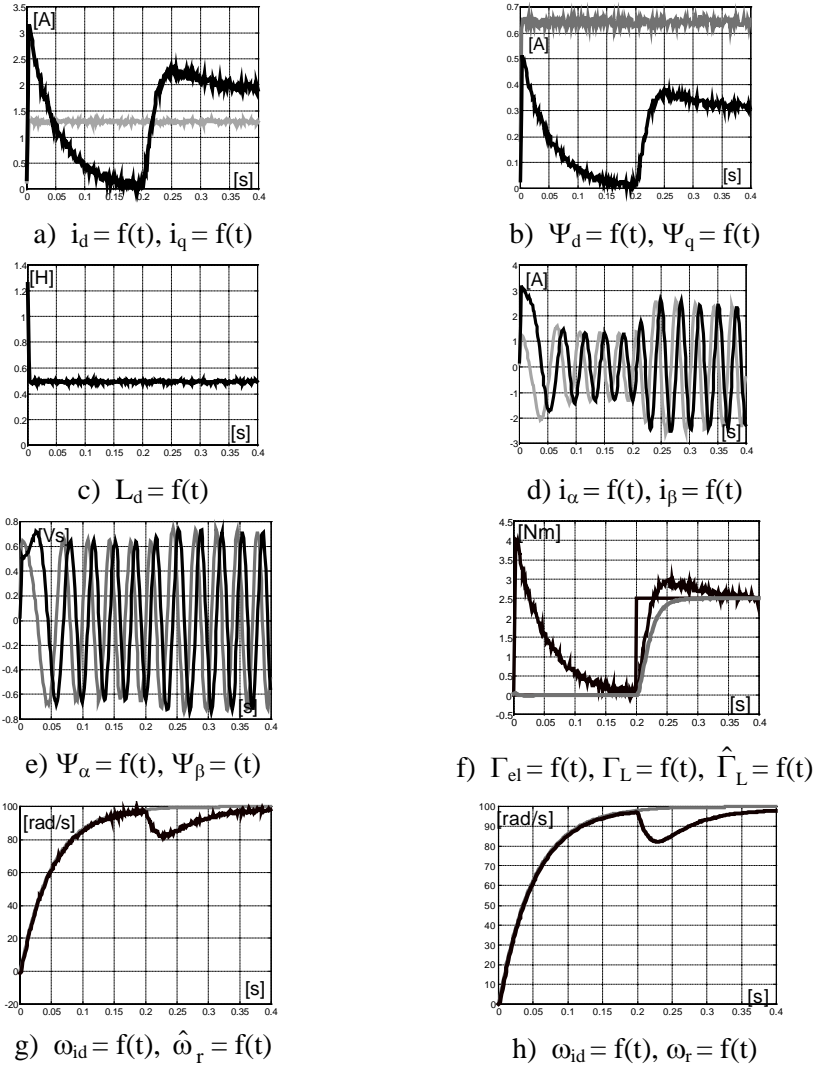


Fig. 4.1.2 Vector control with  $i_d = \text{const}$

In all the figures the subplots (a) and (b) show the demanded and real values of the current components and real values of the magnetic flux components in the d, q rotor fixed frame. The changes of the direct inductance,  $L_d$  due to changes in the direct current,  $i_d$ , are shown in subplot (c). Subplots (d) and (e) show the stator currents and magnetic flux components viewed in the stator fixed  $\alpha, \beta$  frame. Subplot (f) shows the initially exponentially decaying motor torque and the applied load torque,  $\Gamma_L$  together with its estimate  $\hat{\Gamma}_L$ . The estimated values of the load

Torque from the observer may just be seen to follow the step increase in load torque at  $t = 0,2$  s with a small dynamic lag according to  $T_{s0} = 50$  ms. This gives rise to the small transient reduction in the rotor speed just after  $t = 0,2$  s. The speed estimate from the filtering observer together with the ideal speed response are shown in subplot (g). Apart from the transient due to a small lag in load torque estimation, the required first order speed dynamics with a prescribed time constant of  $T_{\omega} = 0,05$  s is evident from the motor speed response, which are shown in subplot (h) together with the ideal one.

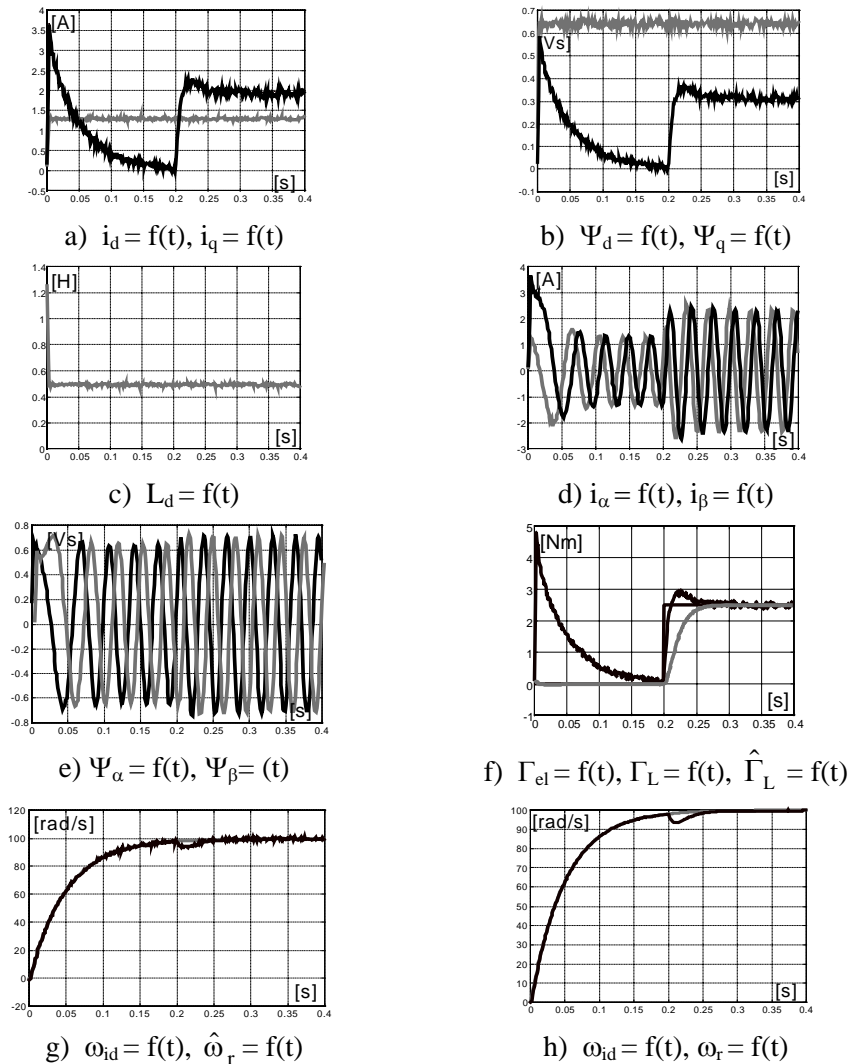


Fig. 4.1.3 Vector control with  $i_d = \text{const}$  and MRAC

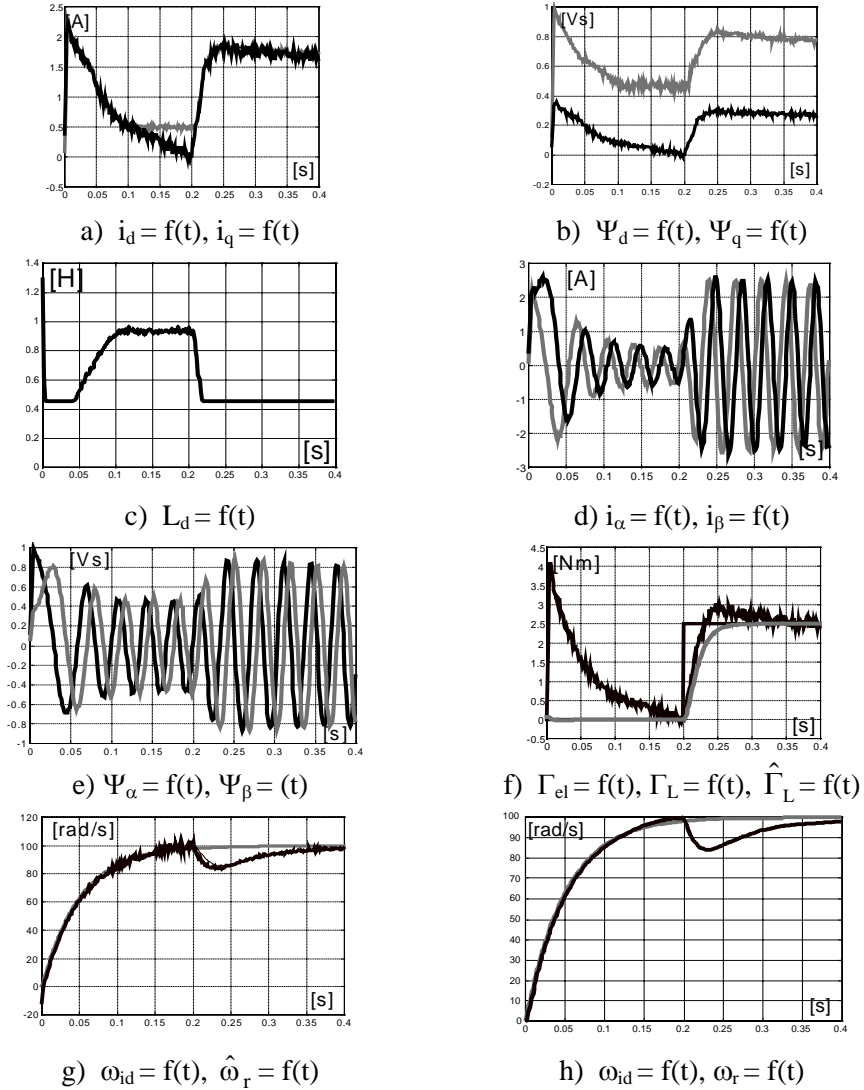


Fig. 4.1.4 Current  $d, q$  angle control for maximum power factor

The control law parameters for all the simulations were as follows: master control law closed-loop time constant:  $T_o=0,05$  s; observer filtering time constant:  $T_{s0}= 0,05$  s; pseudo sliding mode observer model correction loop gain:  $K_{sm}=16000$ . In all these simulations perfect matching between the motor parameters and those assumed in the control laws and observers are assumed.

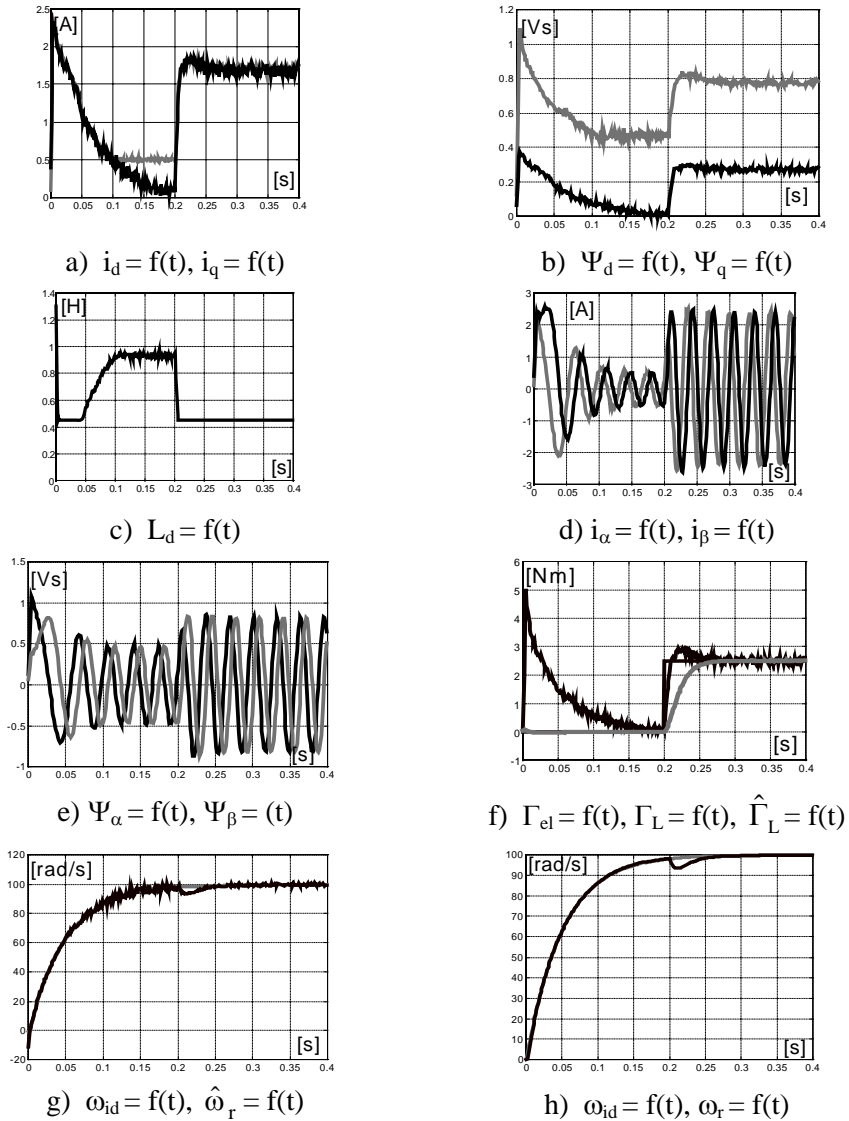


Fig. 4.1.5 Current  $d, q$  angle control for maximum power factor with MRAC

A substantial improvement of the drive performance for both control algorithms can be seen when the MRAC outer loop is added (Fig. 4.1.3 and Fig. 4.1.5). While compensation of the angular speed drop due to application of nominal load torque takes approximately 0,2 s for the basic algorithms, this is

compensated in 0,05 s by the MRAC outer control loop. Also the absolute value of speed drop is nearly four times lower with the MRAC augmentation, when compared with the basic system combining forced dynamic control and the standard vector control.

#### **4.1.6 Conclusions and Recommendations**

The simulation results of the proposed new control method for electric drives employing RSM with forced dynamics show a good agreement with the theoretical predictions. The only substantial departure of the system performance from the ideal is the transient influence of the external load torque on the demanded rotor speed. Although this effect is not too serious, its considerable reduction with the aid of a MRAC based outer control loop were verified.

Some preliminary investigations to test the robustness to motor parameter mismatches show promising results which are not published here due to space limitations, especially when the amount of results is doubled when the MRAC outer control loop is added. Further investigations of robustness, however, should be carried out, particularly with regard to dynamic load parameter mismatches and time varying external load torques.

It is highly desirable to further investigate the proposed control strategy experimentally with a new ALA RSM described in [8].

#### **4.1.7 References**

- [1] I., BOLDEA, A. S., NASAR: '*Vector Control of AC Drives*'. CRC Press. Boca Raton, 1992.
- [2] S. V., DRAKUNOV, D. B., IZOSIMOV, A. G., LUK'YANOV, V. A., UTKIN, V. I., UTKIN: '*The block control principle, I, II*'. *Automation and Remote Control*, Vol. 45, pp. 601-609, No. 5, 1990.
- [3] V. I., UTKIN: '*Method of separation of motions in observation problems*'. *Automation and Remote Control*, Vol. 44, pp. 300-308, No. 12, 1990.
- [4] V. I. UTKIN: '*Sliding Modes in Control and Optimisation*'. Springer-

Verlag, Berlin, 1992.

- [5] S. J., DODDS, V. A., UTKIN, J., VITTEK: ‘*Self Oscillating, Synchronous Motor Drive Control System with Prescribed Closed-Loop Speed Dynamics*’. Proceedings of 2<sup>nd</sup> EPE Chapter Symposium, Nancy, France, June 1996, pp. 23-28.
- [6] S. J., DODDS, S. J., J., VITTEK: ‘*Synchronous Motor Drive with Prescribed Closed-loop Speed Dynamics Employing a Two-phase Oscillator*’. Proceedings of EDPE’96 conference Vol. 1, High Tatras, Slovakia, Oct. 1996, pp. 80 - 88
- [7] S. J., DODDS, J., VITTEK, S., SEMAN: ‘*Implementation of a Sensorless Synchronous Motor Drive Control System with Prescribed Closed-Loop Speed Dynamics*’. Proceedings of SPEEDAM’98 Symposium, Sorrento, Italy, June 1998, pp. P4-5 – P4-10
- [8] M., LICKO, V., HRABOVCOVA: ‘*Design Aspects of Axially Laminated Anisotropic Reluctance Synchronous Motor*’. Proceedings of TRANSCOM’99 conference, section 3, University of Zilina, Slovakia, May 1999, pp. 39 – 45.

## Appendix

Reluctance synchronous motor parameters:

Nominal voltage	380 V (for Y)	Stator resistance	$R_s = 8.62 \Omega$
Nominal current	2.01 A	Quadr. inductance	$L_q = 161.8 \text{ mH}$
Rated power	400 W	Number of polpairs	$p = 2$
Inverter dc voltage	550 V	Moment of inertia	$J = 0.0021 \text{ kgm}^2$

Polynomial approximation of the direct inductance  $L_d(i_d)$  in the working range of stator currents:  $L_d = 0,2913.i_d^2 - 1,0755.i_d + 1,4$  [H; A] with condition: if  $L_d < 0,45$  then  $L_d = 0,45$ .

## Acknowledgements

The authors wish to thank the **European Commission, Brussels**, for funding the **INCO COPERNICUS programme No.960169 ‘Ucodrive’** and **Slovak Grant**

**Agency VEGA** for funding research programme **No.1/6111/99** which enabled us to present these results.